Shot-profile Dip Moveout

Biondo Biondi and *Shuki Ronen*

ABSTRACT

All the known Dip Moveout (DMO) methods require the seismic data to be sorted in midpoint and half offset coordinates. In this paper a DMO method for shot profiles is proposed.

The DMO operator in shot profiles is defined in a way analogous to the well known operator in constant-offset sections. The two operators are found to be equivalent and to have impulse responses with the same projection on the zero offset plane, i. e. the stacking plane. Therefore the application of DMO in constant-offset sections or in shot profiles gives the same stacked section. DMO transforms the shot profiles to zero offset data to which may be applied any post stack migration.

Unfortunately the shot-profile DMO operator is space and time variant; thus its direct application would be computationally expensive. Instead, after a logarithmic transformation of both the coordinates the operator becomes time and space invariant, and then the procedure may be performed efficiently as a convolution in Fourier domain.

The performance of the algorithm is shown in field data examples and the results are compared with the conventional DMO in constant-offset sections.

The sensitivity to inaccurate NMO velocity and the possibility of performing residual velocity analysis is also analyzed with the help of some synthetics examples.

INTRODUCTION

Dip Moveout correction is a well-known method that images dipping reflectors that otherwise would be lost in the conventional stacking procedure. Many of the known algorithm for prestack full migration operate in shot profiles but all prestack partial migration methods require sorting the data to constant-offset sections. In this paper a method is proposed to perform DMO in shot profiles.

Shot profiles have the theoretical advantage that the data was recorded from the same single physical experiment, it is then possible to adapt the processing to acquisition geometry changes

or velocity profile variations. A practical advantage is an easier management of the whole data set and a straightforward parallel implementation of the algorithms. Another reason to process the data in field coordinates is that usually profiles are better sampled than constant-offset sections; thus operating in shot profiles often avoid to bother with aliasing problems.

Conventional DMO methods are computationally expensive; the procedure proposed is instead efficiently implemented as a fast convolution in the frequency domain. This is possible after a transformation of coordinates that makes the DMO operator time and space invariant. An advantage to implement the procedure as a fast convolution in shot profiles instead of constant-offset sections is that, if the geometry is constant and the lateral velocity variations are mild along a line, it is possible to compute the DMO operator only once for the whole line.

THE DMO OPERATOR IN SHOT PROFILES

We now derive the DMO operator in shot profiles in a similar way to its equivalent in constant-offset sections (Hale, 1984).

The arrival time t of the reflection from a dipping bed in field coordinates is given by the equation (Claerbout, 1985)

$$t = \sqrt{\frac{4s^2 \sin^2 \alpha + 4sf \sin^2 \alpha + f^2}{v^2}} \tag{1}$$

where s is the distance between the shot and the point where the dipping reflector meets the surface, f is the full offset, α is the dip of the reflector and v is the medium velocity, assumed constant; velocity variations will be discussed in a following section. If we apply to the equation (1) the dip corrected NMO transformation

$$t = \sqrt{t_0^2 + \frac{f^2 \cos^2 \alpha}{v^2}} \tag{2}$$

we get the following well known kinematic relation in zero offset time t_0 and midpoint y

$$t_0 = \frac{2(s + f/2) \sin \alpha}{v} = \frac{2y \sin \alpha}{v}. \tag{3}$$

The dip corrected NMO transformation may be performed as two cascaded processes:

$$\text{NMO} \qquad t = \sqrt{t_n^2 + \frac{f^2}{v^2}} \tag{4}$$

and

$$\textbf{DMO} \qquad t_n = \sqrt{t_0^2 - \frac{f^2 \sin^2 \alpha}{v^2}}. \tag{5}$$

From equation (3) the dip α is easily expressed in the frequency domain as

$$\frac{\sin \alpha}{v} = \frac{k_y}{2\omega_0} = \frac{k_f}{\omega_0}, \tag{6}$$

where ω_0 is the angular frequency corresponding to t_0, k_f and k_y are the wave numbers of the transformed full offset and midpoints. Substituting the last equation in equation (5) we finally find the change of variables that performs DMO in shot profiles

$$t_n = \sqrt{t_0^2 - \frac{f^2 k_f^2}{\omega_0^2}}. \tag{7}$$

The transformation (7) may be performed in the Fourier domain in a similar way to Hale's DMO; if we define

$$A = \sqrt{1 + \frac{f^2 k_f^2}{t_n^2 \omega_0^2}}; \tag{8}$$

to get the Fourier transformed pressure field $P_0(\omega_0, k_f)$, after application of DMO to the shot profile after NMO $p_n(t_n, f)$, we can compute the double integral

$$P_0(\omega_0, k_f) = \int \int dt_n df A^{-1} e^{i\omega_0 t_n A} \, e^{ik_f f} p_n(t_n, f). \tag{9}$$

This operator is not only time variant but also space variant and thus its application is more expensive than its equivalent in constant-offset sections.

One example of the direct application of the operator in Fourier domain to four impulses is shown in Figure 1. As it is clear from the figure, and it is possible to derive with a stationary phase approximation of the double integral in (9), the impulse response of the DMO operator in shot profiles is the ellipse

$$\left(\frac{t}{t_0}\right)^2 + \left(\frac{f - f_0}{f_0}\right)^2 = 1, \tag{10}$$

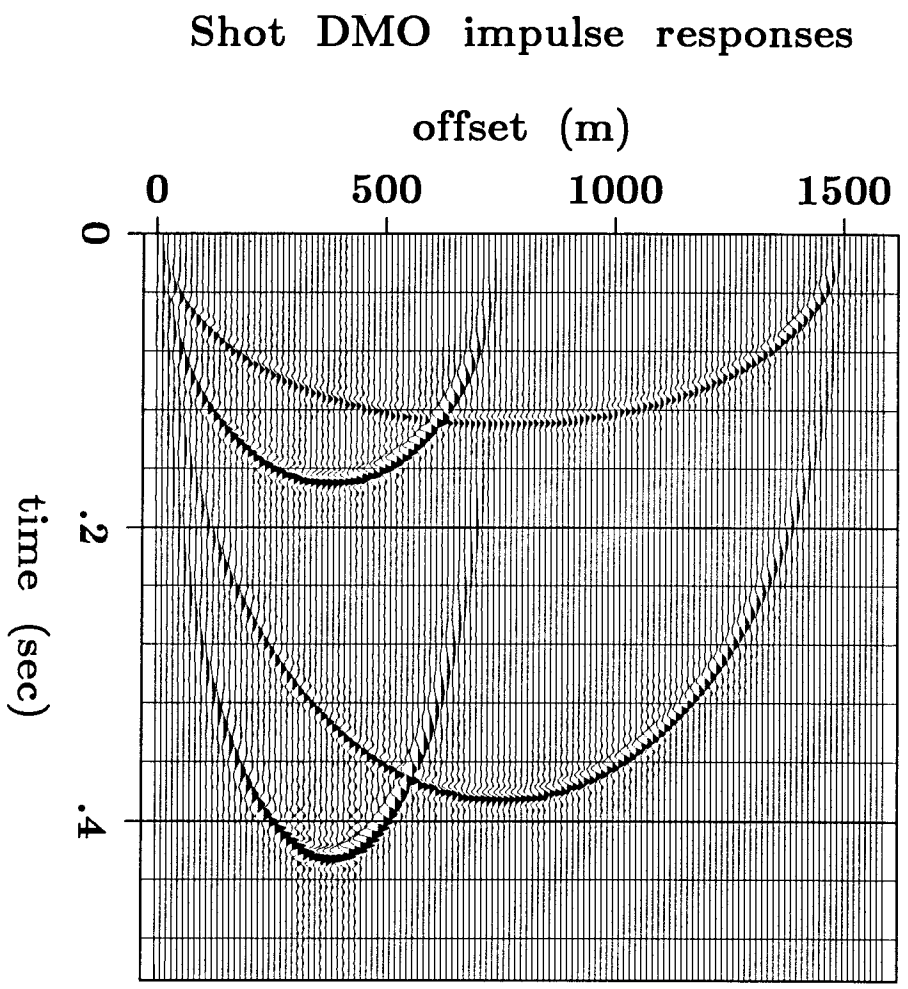

Figure 1: Shot profile DMO impulse response to four spikes. This figure was obtained by numerically computing the double integral in equation (9). The curves are ellipse of equation (10) and passing through the origin.

where t_0 is the impulse time and f_0 is the impulse full offset. For different t_0 and f_0 the axes of the ellipse change but the curve always passes through the origin. This impulse response could have been derived by a change of variables from the conventional "smile" in constant-offset sections (Deregowski and Rocca, 1981)

$$\left(\frac{t}{t_0}\right)^2 + \left(\frac{y - y_0}{h}\right)^2 = 1, \tag{11}$$

where $y = s + f/2$ is midpoint and $h = f/2$ is half offset.

Actually the two impulse responses have the same projection on the zero offset plane; this

means that an impulse in the data will produce the same result in the stacked section using either DMO operator. In other words applying DMO to the data in constant-offset sections or in shot profiles will give the same stack; for the stacked section the two operators are perfectly equivalent.

The application of DMO transforms the shot profile into a real zero offset section, it is then possible to process it with post stack algorithm, as for example, a post stack migration.

A time and space invariant DMO

The DMO operator in shot profiles that we found in the preceding section is time and space variant. Its computational cost is overwhelming. Instead after an appropriate change of variables of both the coordinates it becomes invariant. The right change of variables is of logarithmic type and was proposed by Bolondi et al. (1982) and Wang et al. (1985). Let

$$\tau = \log(t) \qquad \text{and} \qquad \phi = \log(f) \tag{12}$$

in the expression (10). We will then have the curve

$$(\exp(\tau - \tau_0))^2 + (\exp(\phi - \phi_0) - 1)^2 = 1, \tag{13}$$

that is the impulse response of the operator in the new coordinates. This curve now depends only on the differences $(\tau - \tau_0)$ and $(\phi - \phi_0)$, therefore the operator is invariant. The convolution with this impulse response is efficiently performed with a multiplication in Fourier domain.

The proposed algorithm of DMO in shot profiles is thus composed of three basic step. The first is stretching the data according to transformations (12); the second is convolving the stretched data with the invariant operator in the Fourier domain. The final step is to transform back the data to the original time and offset space with an inverse change of variables.

One theoretical problem for the application of the algorithm is that the logarithmic transformation of variables is not defined at time zero and at zero offset. In practice the first time samples are seldom interesting and we will usually never have a zero offset recording.

Field data results

The performance of the DMO algorithms was tested with a data set from the Gulf of Mexico. Figure 2 and 3 show the whole stacked sections obtained with and without the application of DMO in shot profiles.

The following figures show a window of the stack; where the differences owing to the application of DMO are more evident. The goal of the DMO here is to properly image the fault plane reflection and the tails of the diffraction hyperbolas. In Figure 4 a conventional stack is shown. The fault

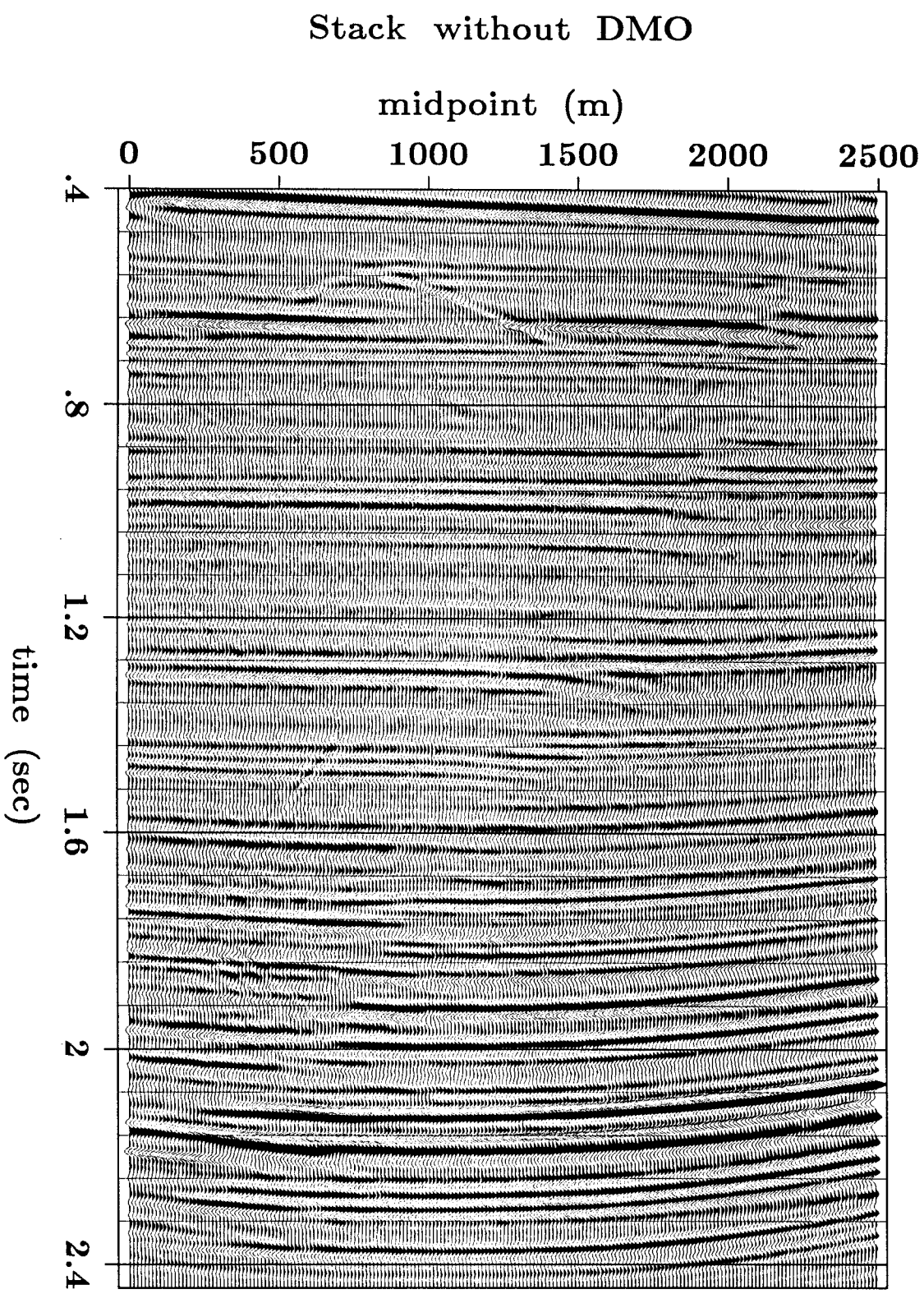

Figure 2: Stacked section of a data set from Gulf of Mexico. This stack was obtained without the use of DMO.

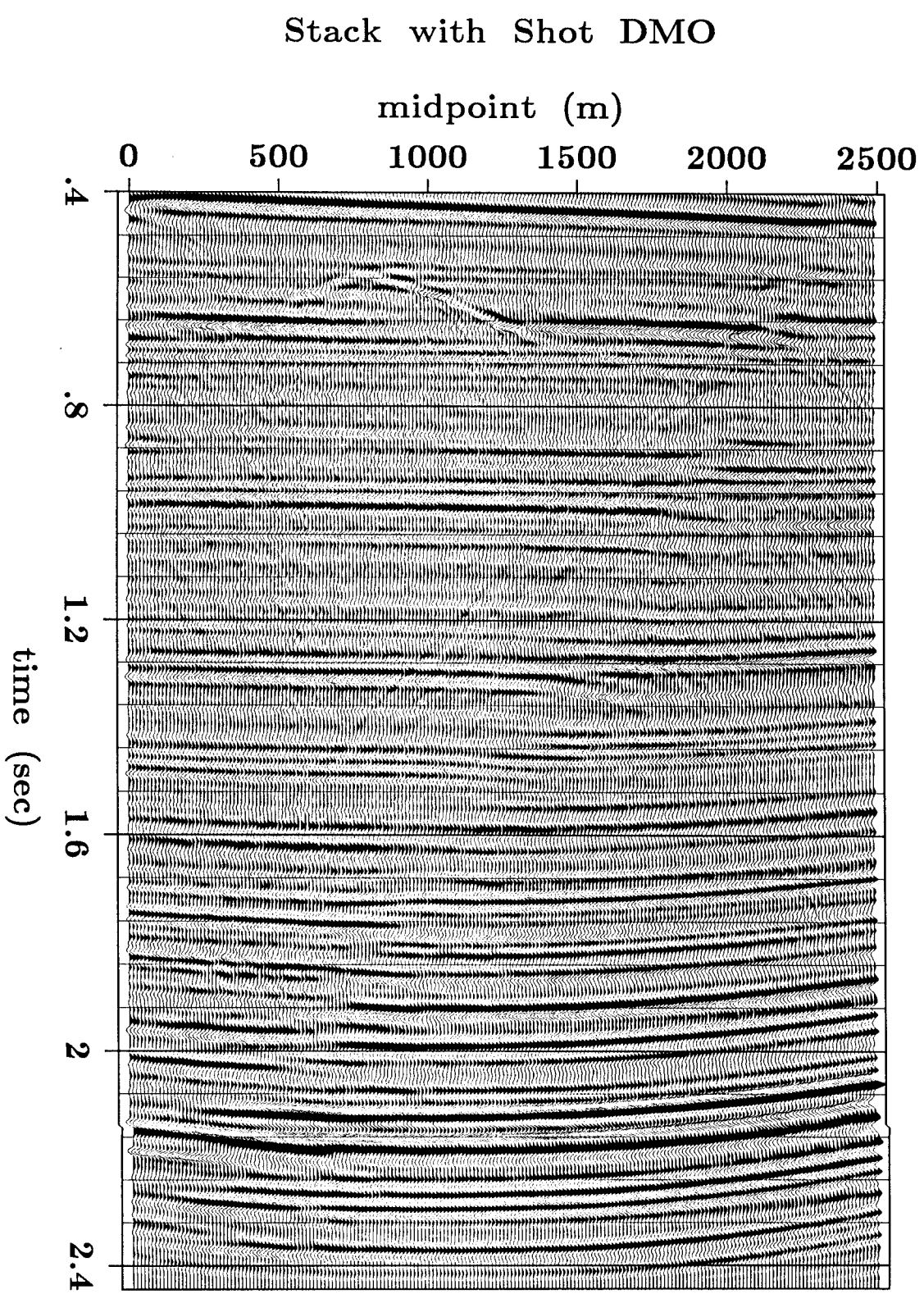

Figure 3: Stacked section of the same data set of Figure 2. This stack was obtained after DMO in shot profiles. Shot profile DMO has imaged the dipping events in the stack.

reflection has completely disappeared and the diffraction hyperbolas are weak. Instead in the stack after applying DMO in shot profiles (Figure 5), the fault reflection is present and the diffractions are easily noticed. Figure 6 shows for control the stacked section after applying DMO in constant-offset sections. The two results in Figure 5 and Figure 6 are almost identical, there is only a slight difference in the shallow part where DMO in shot profiles has better imaged some diffraction hyperbolas.

SHOT DMO AND RESIDUAL VELOCITY ANALYSIS

For a practical application of the shot-profile DMO it is interesting to know if it is correct to perform a residual velocity analysis and a consequent residual NMO (RNMO) after DMO. The reason is that velocity analysis is more accurate after DMO than before, because the effects of the dip on the stacking velocity have been removed.

The application of a RNMO after DMO introduces some error because in the derivation of DMO in shot profiles, equations (4) and (5), the DMO process follows NMO and the two operators do not commute. We want to compare the error due to the application of the operators in the wrong sequence for the shot-profile DMO and the constant-offset DMO.

In the appendix it is shown that NMO and DMO do not commute because the DMO shift is dip dependent. The error introduced applying a RNMO after DMO depends mainly on the DMO sensitivity to inaccuracies in NMO velocity ; more exactly it depends on the DMO sensitivity to incorrect dip information in the data and on the dip error introduced by an inaccurate NMO velocity.

In both DMO methods the shift depends on the dip in the same way, and therefore their sensitivity to a dip error should be equivalent. On the contrary, an error in the NMO velocity has more influence on the dips in shot profiles than in constant-offset sections. Consequently shot-profile DMO is more sensitive to errors in NMO velocity than DMO in constant-offset sections.

The following synthetic examples confirm the theoretical result, but they also show that a residual velocity analysis and RNMO are still feasible and helpful after shot-profile DMO.

The synthetic data set was generated assuming a flat reflector and one bed dipping at 60°, in a medium of constant velocity equal to 2000 (m/sec), the shot interval was assumed to be 25 meters and the group interval equal to 12.5 meters. In Figure 7 a CDP gather and the correspondent contour plot of the semblance function of the stacking slowness and time are shown. The upper hyperbola is the dipping bed reflection and the lower the flat bed reflection. Figure 8 shows the same CDP gather after NMO with the correct velocity followed by DMO and inverse NMO. The plots on the left are obtained after the application of shot-profile DMO and the ones on the right after constant-offset DMO. The corresponding semblance plots for velocity analysis are shown too. The results after a correct NMO are equivalent. Note that in the CDP gather after constant-offset

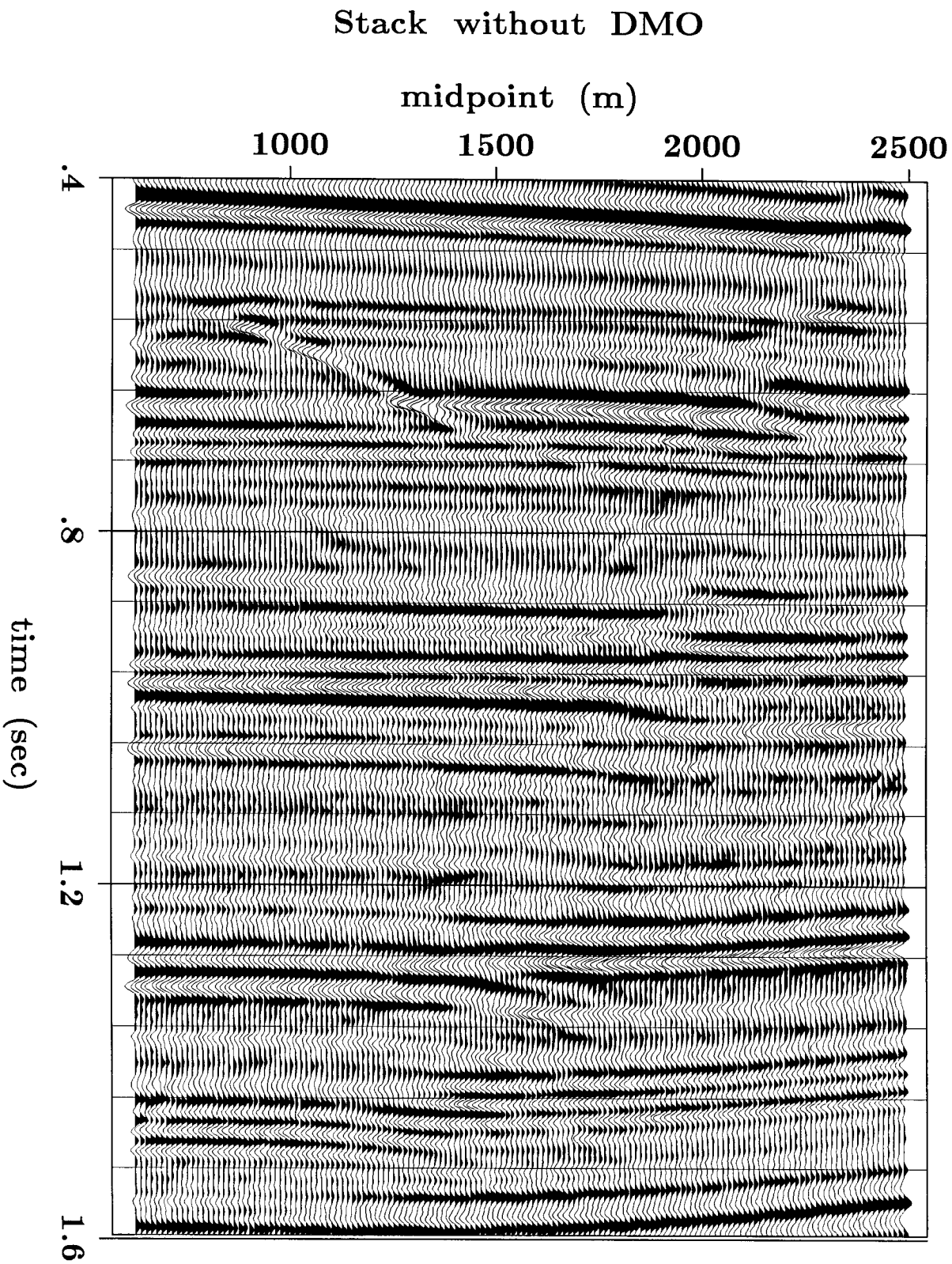

Figure 4: Window of the section in Figure 2. The stack without DMO has suppressed the dipping events.

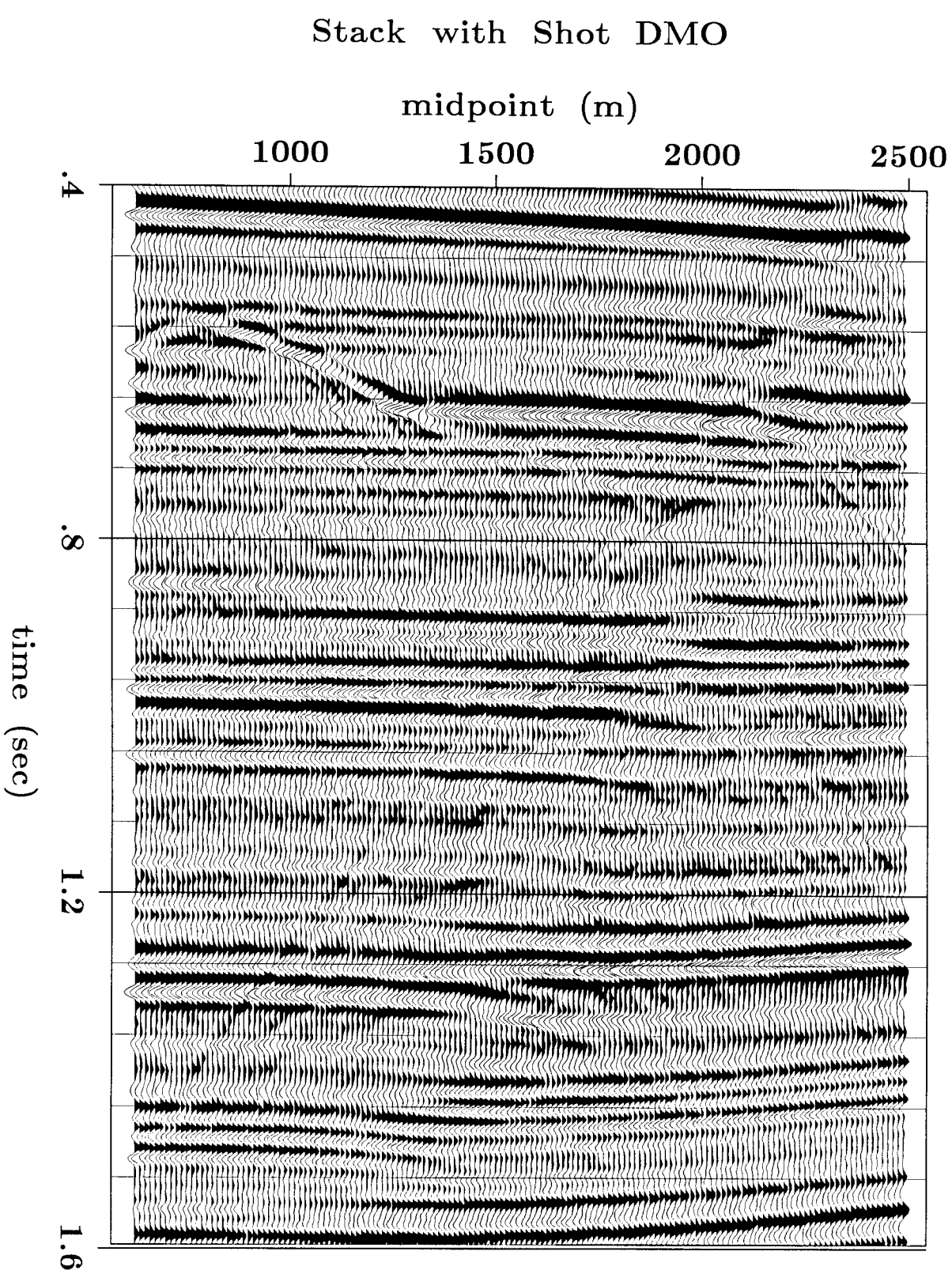

Figure 5: Window of the section in Figure 3. The DMO in shot profiles has restored the dipping events like the fault plane reflection and the diffraction hyperbolas.

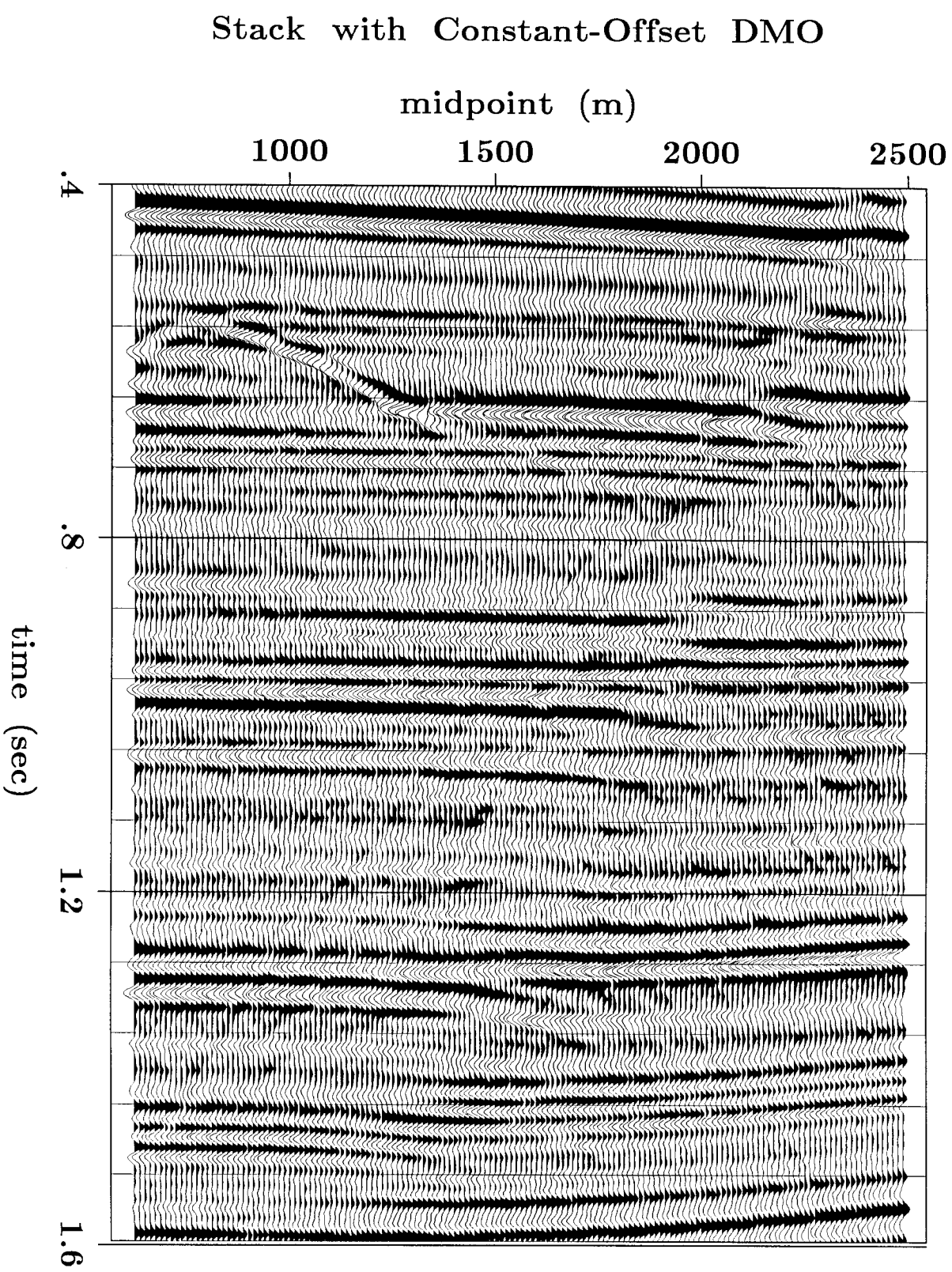

Figure 6: Same window of the data as in Figure 4 and 5, but the data was stacked after applying conventional DMO in constant offset sections. It is hardly possible to notice any difference between this figure and Figure 5.

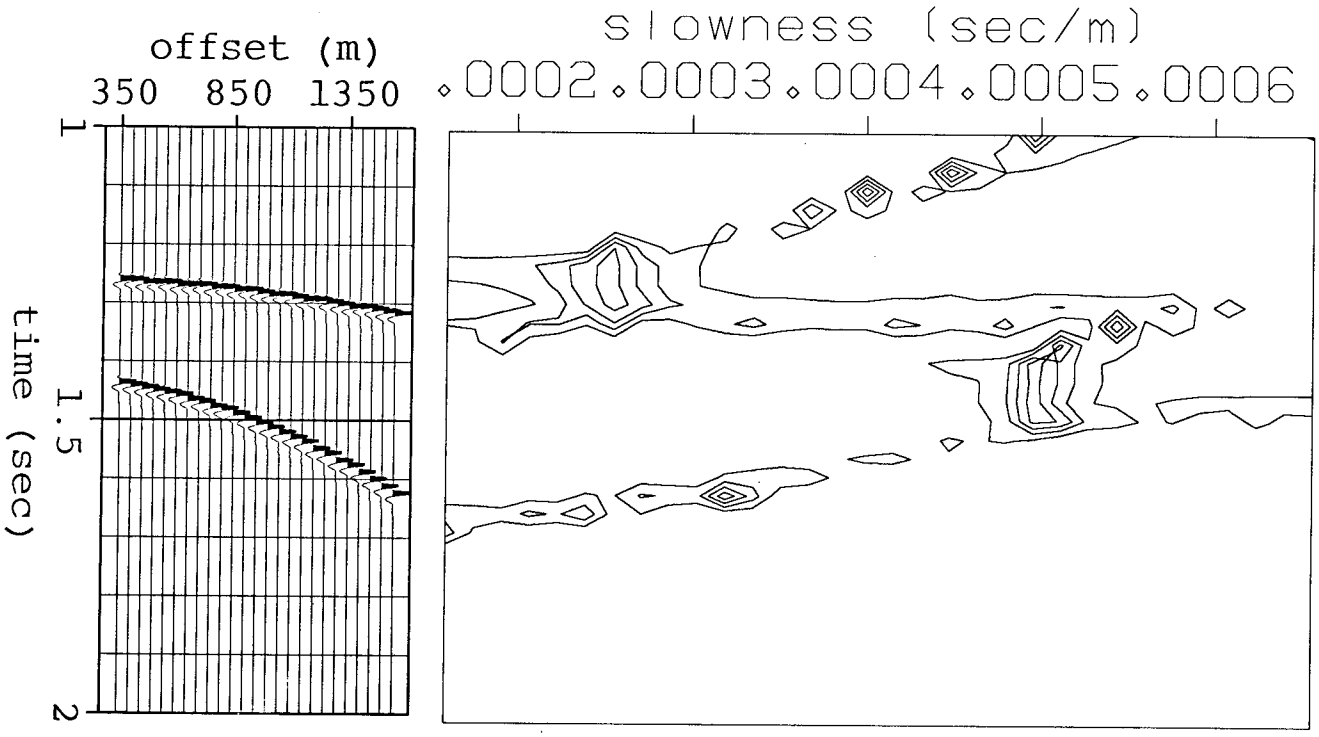

Figure 7 : Synthetic CDP gather and correspondent semblance function for velocity analysis. The upper hyperbola is the reflection of a 60 degree dipping bed and the lower one of a flat reflector. The velocity of the medium was supposed constant and equal to 2000 (m/sec) (slowness equal to .0005 (sec/m)).

DMO some aliasing noise is present.

The sensitivity to an inaccurate NMO velocity is analyzed in Figure 9 and Figure 10. They show the same CDP as in Figure 8 but with different NMO velocities. In Figure 9 the NMO velocity is 1800 (m/sec), 10% lower than the correct one, and in Figure 10 is 2200 (m/sec), 10% higher than the right one. The residual velocity analysis after shot-profile DMO is slightly off by about 3% in both cases; on the contrary the residual velocity analysis after DMO in constant-offset sections is almost perfect.

The stacks corresponding to the precedent CDP gathers are shown in Figure 11 and Figure 12. The stacking velocity was always chosen to be the right one for the flat reflector, that is the medium velocity. The stack after DMO in shot profiles is somewhat more sensitive to errors in NMO velocity.

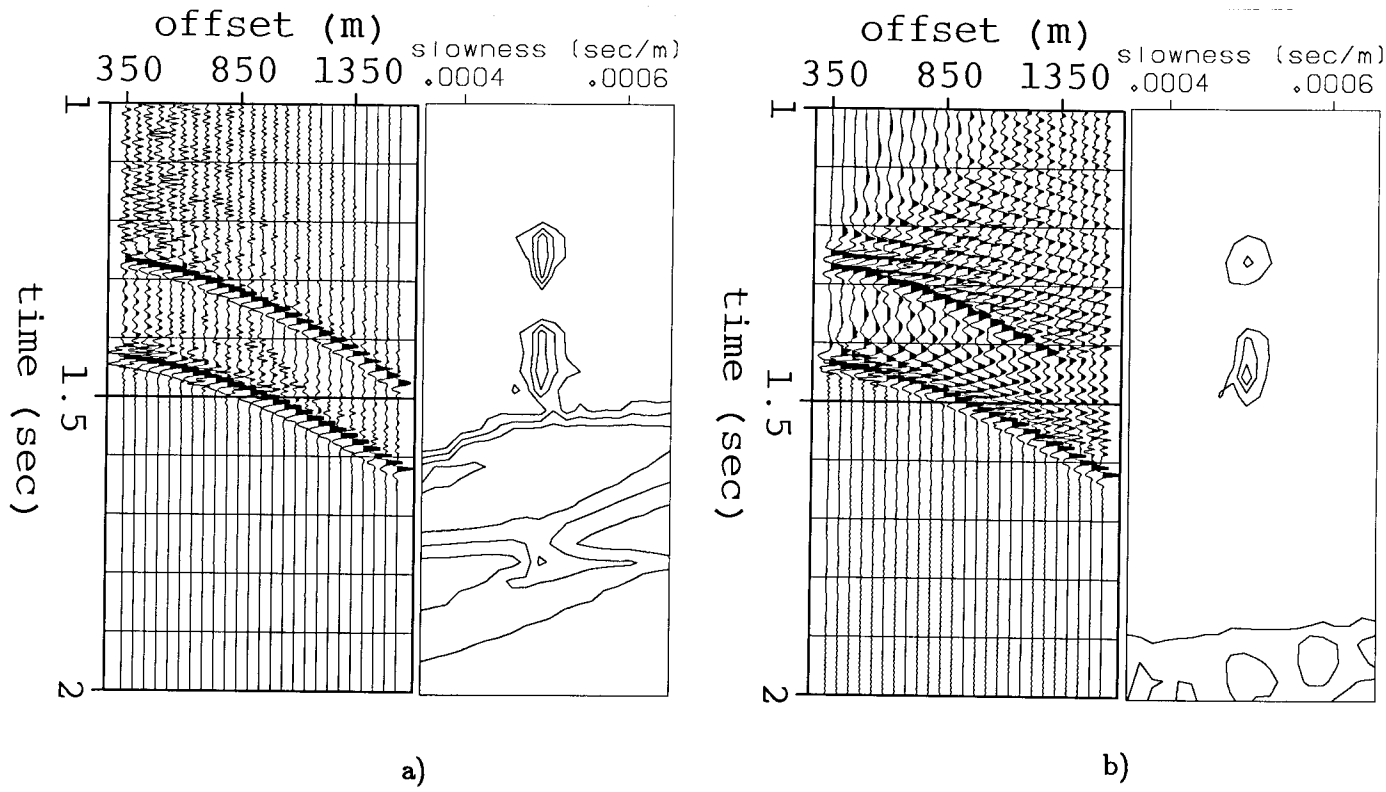

Figure 8: The same CDP gather of Figure 7 after NMO, DMO and inverse NMO: a) with shot profile DMO, b) with constant-offset DMO. The velocity used for NMO is the correct one (2000 (m/sec)). The correspondent velocity analyses are shown next to the gathers. Because the NMO velocity is correct both methods correct the dip effect perfectly. In the gather after constant offset DMO there is some aliasing noise that will disappear in the stack.

DMO AND VELOCITY VARIATION

Constant-offset DMO has been generalized to handle with a good approximation velocity variations with depth (Bolondi et al, 1984; Hale, 1984). It is likely that the same considerations may be extended to generalize the shot-profile DMO.

On the other hand a generalization to lateral velocity variation of the conventional DMO is more difficult because it would result in a space variant operator, with a consequent important increase in computational cost. This is a problem in constant-offset sections because all the line is Dip Moved Out at the same time. A shot profile is only a small part of the data and it depends on a well localized part of the subsurface; it is then possible to adapt the processing to lateral velocity variations, with a good approximation, leaving the operator space invariant within a single shot profile, but changing it from shot to shot.

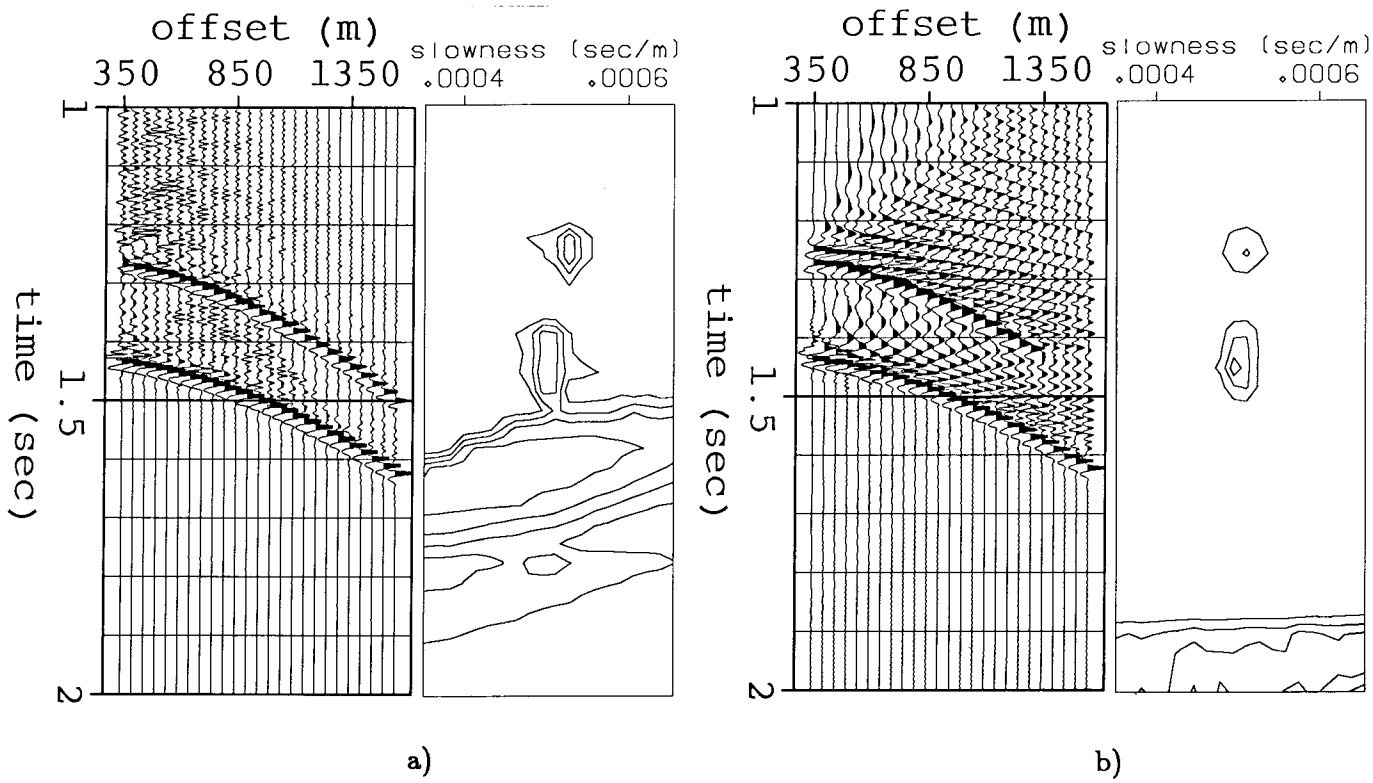

Figure 9: The same CDP gathers of the previous figures but now with a NMO velocity equal to 1800 (m/sec), that is 10% lower than the correct one: a) with shot profile DMO, b) with constant-offset DMO. The conventional DMO is less sensitive to errors in NMO velocity than DMO in shot profiles. The error in the residual velocity analysis after shot profile DMO is about -3%.

CONCLUSIONS

The proposed algorithm has all the advantages of processing the data in field profiles, and it produces equivalent stacked sections to those produced by DMO in constant-offset sections, as has been shown with field data examples. The possibility to perform a residual velocity analysis and a residual NMO after shot-profile DMO has been shown. It is then possible to conclude that all prestack processing can be performed in shot profiles without resorting the data in midpoint and offset coordinates; actually only some CDP gathers used for velocity analysis need to be sorted out.

The sensitivity of the method to depth and lateral velocity variation must be analyzed, but it seems that a shot profile is a more flexible domain than constant offset sections to approximate the necessary modification to the DMO operator.

The algorithm, thanks to the logarithmic change of variables, is faster than DMO in constant-

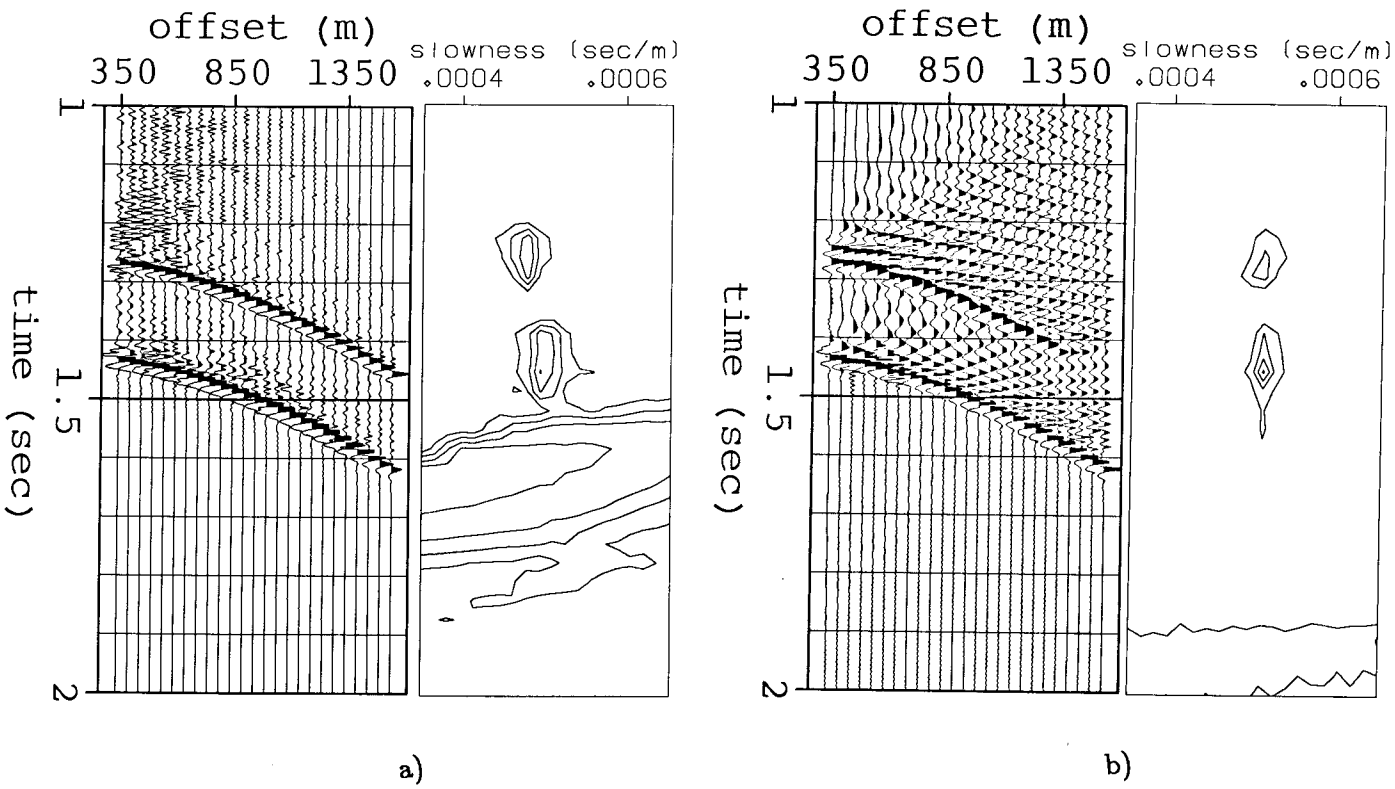

Figure 10: The same CDP gathers of the previous figures but now with a NMO velocity equal to 2200 (m/sec), that is 10% higher than the correct one: a) with shot profile DMO, b) with constant-offset DMO. The error in the residual velocity analysis after shot profile DMO is about +3%.

offset sections. Of course the change of variables would work also for a constant-offset DMO; but one computational advantage to work in shot profiles is the possibility to precompute the operator and then use it for all the shot profiles of the survey.

ACKNOWLEDGMENTS

We would like to thank Stew Levin for many helpful discussion and Chevron Oil Company for releasing the data.

REFERENCES

Biondi, B., and Claerbout, J.F. , 1985, Pseudounitary NMO: SEP 44, p.75.

Bolondi, G., Loinger, E., and Rocca, F., 1982, Offset continuation of seismic sections: Geophysical Prospecting, v.30, p.813-826.

Bolondi, G., Loinger, E., and Rocca, F., 1984, Offset continuation in theory and *in practice:*

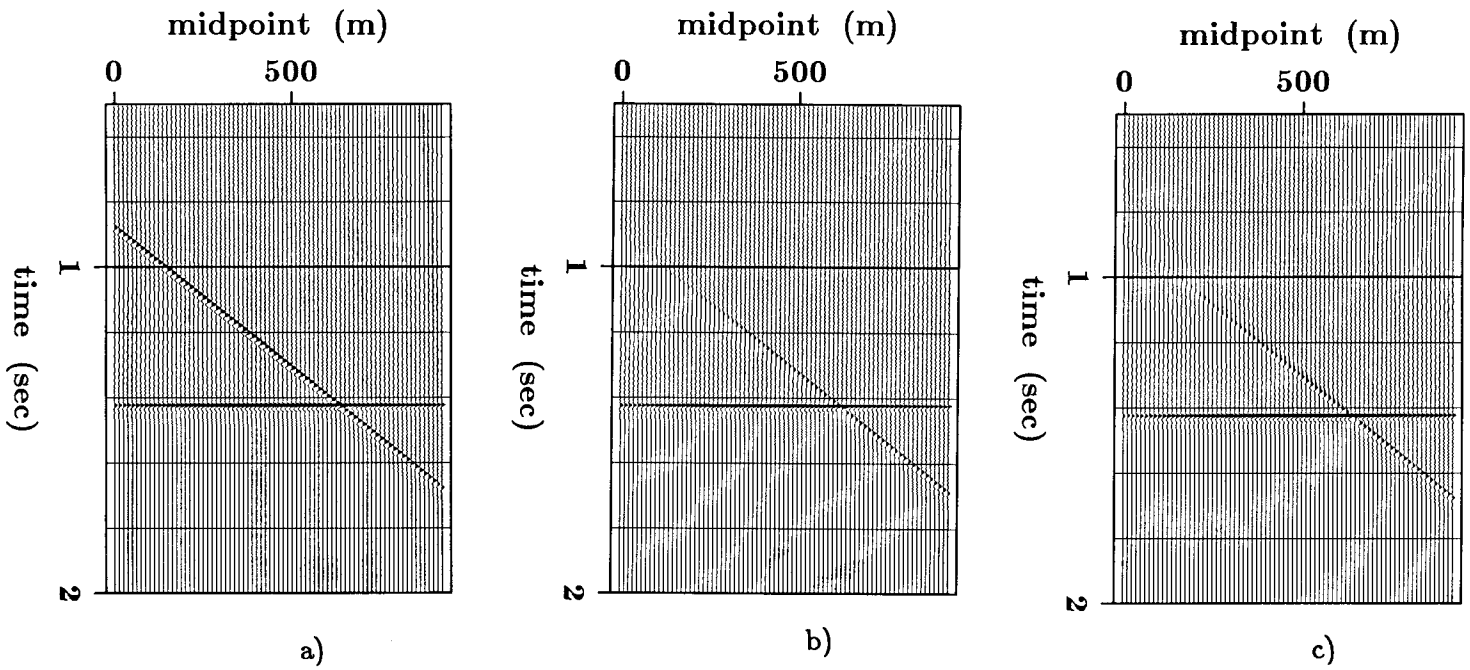

Figure 11: Three stacks of the synthetic data set using the shot profile DMO. The stacks were obtained using different NMO velocities: a) NMO with the correct velocity, b) with a 10% lower velocity and c) with a 10% higher velocity. The result degrades slightly owing to an uncorrect NMO velocity.

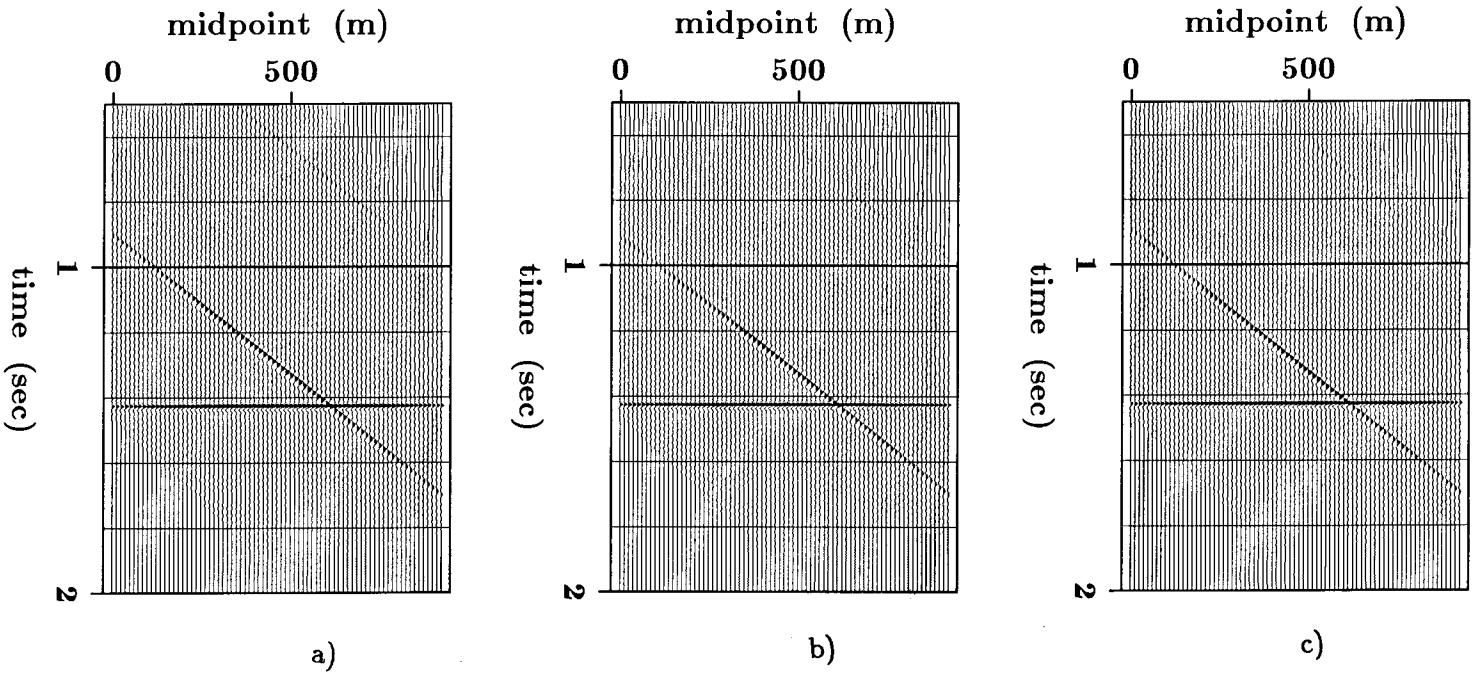

Figure 12: Three stacks of the synthetic data set using the constant offset DMO. The stacks were obtained using different NMO velocities: a) NMO with the correct velocity, b) with a 10% lower velocity and c) with a 10% higher velocity. Note that the aliasing noise visible in the gathers has disappeared in the stacks.

Geophysical Prospecting, v.32, p.1045-1073.

Claerbout, J.F., 1985, Imaging the Earth Interior: Blackwell Scientific Publication, p. 162-163.

Deregowski, S.M., and Rocca, F. 1981, Geometrical optics and wave theory of constant-offset sections in layered media: Geophysical Prospecting, v.29, p.384, 406.

Hale, I. D., 1984, Dip-moveout by Fourier transform: Geophysics, v. 49, 741-757

Wang, S.Y., Pan, N.D., and Gardner, G.H.F., 1985, Dip-moveout expressed as an invariant convolution: Seismic Acoustic Laboratory, University of Houston, Semi-Annual Progress Review, 16, 260-276.

APPENDIX

In this appendix we want to show that the error introduced applying the three step process NMO, DMO and RNMO is owed mainly to the DMO sensitivity to an inaccurate NMO velocity. We show it for constant velocity v and reflections of a dipping bed of dip α.

The dip corrected NMO transformation

$$t = \sqrt{t_0^2 + \frac{f^2 \cos^2 \alpha}{v^2}} \tag{A1}$$

may be performed as three cascaded processes:

NMO
$$t = \sqrt{t_1^2 + \frac{f^2}{v_1^2}} \tag{A2}$$

DMO
$$t_1 = \sqrt{t_2^2 - \frac{f^2 \sin^2 \alpha}{v^2}} \tag{A3}$$

RNMO
$$t_2 = \sqrt{t_0^2 + \frac{f^2}{v_2^2}} \tag{A4}$$

where v_1 and v_2 are such that

$$\frac{1}{v^2} = \frac{1}{v_1^2} + \frac{1}{v_2^2}. \tag{A5}$$

Here we assume that v_1 is greater than v, the extension to the other case is immediate. The three step procedure is exact if the term $\beta = \sin\alpha / v$ is the correct one; in practice β is estimated from the data using the relation

$$\beta = \frac{\sin \alpha}{v} = \frac{k_y}{2\omega_0} = \frac{k_f}{\omega_0}; \tag{A6}$$

when the input to the DMO process is not the data transformed with the right NMO velocity v but with the larger velocity v_1. The estimated β will be different from the correct one and equal to β_1. We can express the ideal and correct result of the whole process as

$$\mathbf{res} = RNMO\ DMO(\beta)\ NMO\ \mathbf{data}, \tag{A7}$$

and the wrong one and actually computed as

$$\mathbf{res_1} = RNMO\ DMO(\beta_1)\ NMO\ \mathbf{data}. \tag{A8}$$

All the operators are linear and the error may be the expressed as

$$\mathbf{err} = \mathbf{res} - \mathbf{res_1} = RNMO\ (DMO(\beta) - DMO(\beta_1))\ NMO\ \mathbf{data}. \tag{A9}$$

Because the NMO operators are close to unitary, or better pseudounitary (Biondi and Claerbout, 1985), the error depends mainly on the difference $DMO(\beta) - DMO(\beta_1)$.